



U.S. DEPARTMENT OF
ENERGY

DOE/SC-ARM/TR-088

MMCR Calibration Study

J Mead

March 2010



DISCLAIMER

This report was prepared as an account of work sponsored by the U.S. Government. Neither the United States nor any agency thereof, nor any of their employees, makes any warranty, express or implied, or assumes any legal liability or responsibility for the accuracy, completeness, or usefulness of any information, apparatus, product, or process disclosed, or represents that its use would not infringe privately owned rights. Reference herein to any specific commercial product, process, or service by trade name, trademark, manufacturer, or otherwise, does not necessarily constitute or imply its endorsement, recommendation, or favoring by the U.S. Government or any agency thereof. The views and opinions of authors expressed herein do not necessarily state or reflect those of the U.S. Government or any agency thereof.

MMCR Calibration Study

Submitted by

ProSensing Inc.
107 Sunderland Road
Amherst, MA 01002-1098, USA

March 2010

Work supported by the U.S. Department of Energy,
Office of Science, Office of Biological and Environmental Research

Contents

1.0	Radar Range Equation Error Analysis.....	1
1.1	Derivation of the Radar Range Equation for Millimeter Wavelength Cloud Radar	1
1.2	Error Analysis	3
1.2.1	Errors Due to Range and Scattering Volume Estimation.....	4
1.2.2	Transmit Power Measurement Error	4
1.2.3	Receiver Gain Fluctuations	5
1.2.4	Received Power Measurement Errors	6
1.3	Simulated Bias	10
1.3.1	Temperature Dependence on the Index of Refraction of Water.....	11
1.3.2	Propagation Losses.....	11
1.4	Summary of Error Sources.....	12
1.4.1	References	13

Figures

1	Nauru daily calibration showing drift of +0.3 to -1.4 dB from the initial calibration values.....	5
2	Simulated bias of the zeroth spectral moment as a function of the peak signal-to-mean-noise floor level for three spectral widths: 0.2 m/s, 0.6 m/s, and 2.0 m/s; MMCR CI mode, spectral resolution=.066 m/s.....	7
3	Simulated standard deviation relative to mean of the zeroth spectral moment as a function of the peak signal-to-mean-noise floor level for three spectral widths: 0.2 m/s, 0.6 m/s, and 2.0 m/s; MMCR CI mode, spectral resolution=.066 m/s.	8
4	Typical MMCR receiver transfer function.....	9
5	Mean input power estimation error using transfer function applied after computing the mean measured power.	10
6	Temperature dependence of $ K $ at 35 GHz.	11

Tables

1	Receiver gain minimum, maximum, and standard deviation for the Boundary-Layer mode for the five MMCR installations.....	5
2	Summary of calibration error sources in WACR.	13

1.0 Radar Range Equation Error Analysis

1.1 Derivation of the Radar Range Equation for Millimeter Wavelength Cloud Radar (MMCR)

Following the development presented in section 5-14 of [1], the total scattering volume radar cross section, σ , can be expressed as:

$$\sigma = \sigma_v V_w = \frac{(4\pi)^3 R^4 P_r}{G_0^2 \lambda^2 P_t} \quad (1)$$

where P_r is the received power at the antenna terminals, P_t is the transmit power, G_0 is the peak antenna gain, and R is the target range. The radar cross section is equal to the backscattering cross section per unit volume, σ_v , times the weighted volume, V_w , illuminated by the radar:

$$V_w = \frac{c\tau}{2l_r} \iint_{\theta, \phi} g(\theta, \phi)^2 d\phi d\theta$$

where $g(\theta, \phi)$ is the normalized antenna gain pattern in azimuth (θ) and elevation (ϕ) and $\frac{c\tau}{2l_r}$ is the effective length of the pulse volume in meters, corrected for finite receiver bandwidth effects through the loss factor, l_r [2], which is 1.5 for a matched filter receiver. Assuming a symmetric, Gaussian antenna beam pattern, V_w can be approximated by [3]

$$V_w = \pi \cdot \frac{c\tau R^2 \theta_{3dB}^2}{l_r 16 \ln(2)} \quad (2)$$

where θ_{3dB} is the antenna's one-way half-power beam width. Substituting (2) into (1) yields

$$\sigma_v = \frac{1024 \ln(2) \pi^2 l_r R^2 P_r}{c \tau G_0^2 \lambda^2 \theta_{3dB}^2 P_t} \frac{m^2}{m^3} \quad (3)$$

From section 5.11.3 in [1], σ_v is related to the cloud reflectivity factor, Z in $\frac{mm^6}{m^3}$, by

$$\sigma_v = 10^{-18} \frac{\pi^5}{\lambda^4} |K|^2 Z \quad (4)$$

where K is a function of the complex index of refraction, n :

$$K = \frac{n^2 - 1}{n^2 + 2}$$

For liquid water at 35 GHz, 0°C , $|K| = 0.94$.

Combining (3) and (4) gives Z as:

$$Z = \frac{1024 \ln(2) l_r \lambda^2 R^2 P_r}{10^{-18} c \tau \pi^3 G_0^2 |K|^2 \theta_{3dB}^2 P_t} \quad \frac{m^2}{m^3} \quad (5)$$

This derivation assumes no appreciable atmospheric attenuation between the radar and the radar and the cloud. These loss factors can be included as total two-way path attenuation factors between the radar and scattering volume, l_a , $1.0 < l_a \leq \infty$ with 1.0 being no attenuation:

$$Z = \frac{1024 \ln(2) l_r \lambda^2 R^2 P_r l_a}{10^{-18} c \tau \pi^3 G_0^2 |K|^2 \theta_{3dB}^2 P_t} \quad \frac{m^2}{m^3} \quad (6)$$

The cirrus mode of MMCR employs binary phase coded pulse compression that increases the effective peak power by N_c , where N_c is the number of bits in the binary phase code. $N_c=16$ for the SGP and TWP MMCRs and 32 for the MMCR in Barrow, Alaska. Thus,

$$Z = \frac{1024 \ln(2) l_r \lambda^2 R^2 P_r l_a}{10^{-18} c \tau \pi^3 G_0^2 |K|^2 \theta_{3dB}^2 P_t N_c} \quad \frac{m^2}{m^3} \quad (7)$$

In the MMCR documentation, the constant values in (7) are lumped into the ‘‘Radar Constant,’’ RC , given by

$$RC = \frac{512 \ln(2) \lambda^2 10^{18} L_{sys}}{P_t G_0^2 \theta_{3dB}^2 \Delta R \pi^3 |K|^2 N_c} \quad \frac{m^2}{m^3} \quad (8)$$

where $c \tau$ is replaced by $2\Delta R$ and $L_{sys} = L_t L_r L_{MF}$ is the product of the transmit path loss (L_t), receiver path loss (L_r), and matched filter loss $L_{MF}=2.3$ dB. Reviewing sections 4.4.1–4.4.3 of [2] shows that L_{MF} is equivalent to l_r , the finite bandwidth loss factor, used in [2]. It is important to note that the filter used in MMCR is a Gaussian digital filter, which is not matched. The theoretical loss of a Gaussian filter when processing a rectangular pulse is 2.3 dB (Fig. 4.8 in [2]).

Re-expressing (7) in dB gives the radar equation for MMCR:

$$dBZ = 20 \log R + 10 \log P_r + 10 \log RC \quad (8)$$

1.2 Error Analysis

Equation (7) can be written to explicitly highlight parameters that have uncertainty:

$$Z = \frac{\Gamma R^4 P_r l_a}{V_w G_0^2 |K|^2 P_t} \frac{m^2}{m^3} \quad (9)$$

Where all of the fixed constants and N_c are lumped into a single variable, $\Gamma = \frac{64\lambda^2}{10^{-18}\pi^2 N_c}$

re-expressing (9) in dBZ gives:

$$\begin{aligned} dBZ = 10\log Z = 10\log \Gamma + 40\log R + 10\log P_r + 10\log l_a - \\ 10\log V_w - 20\log G_0 - 20\log |K| - 10\log P_t \end{aligned} \quad (10)$$

Taking the derivative of (10) with respect to individual parameters yields the sensitivity of dBZ to changes in those parameters:

$$\frac{d(dBZ)}{d(10\log R)} = 4$$

$$\frac{d(dBZ)}{d(10\log P_r)} = 1$$

$$\frac{d(dBZ)}{d(10\log l_a)} = 1$$

$$\frac{d(dBZ)}{d(10\log V_w)} = -1$$

$$\frac{d(dBZ)}{d(10\log G_0)} = -2$$

$$\frac{d(dBZ)}{d(10\log |K|)} = -2$$

$$\frac{d(dBZ)}{d(10\log P_t)} = -1$$

Thus, a +x dB error in received power will result in a +x dB error in dBZ, while a +y dB error in estimating the index of refraction factor, $|K|$, will map into a -2y dB error in dBZ. Note that not all of these parameters vary independently. For example, the illuminated volume increases as the square of the target range and inversely with antenna gain.

The error sources in (8) are summarized below:

- Errors associated with the scattering volume range
- Errors in estimating the volume integral, V_w
- Errors associated with measuring transmit and received power
- Uncertainty in the initial measurement of antenna gain and gain stability over time
- Uncertainty in the index of refraction of water due to temperature variation, causing errors in the assigned value of $|K|$.
- Propagation losses between the radar and cloud, including loss due to water deposition on the antenna.

These errors are considered separately below.

1.2.1 Errors Due to Range and Scattering Volume Estimation

The factor $\frac{R^4}{V_w}$ in (9) can be expanded to $\frac{16 \ln(2) l_r R^2}{\pi c \tau \theta_{3dB}^2} = \Phi \frac{R^2}{\theta_{3dB}^2}$ where Φ is a constant. Assuming that

the received pulse shape is well characterized by the loss factor l_r , as was shown for the W-Band ARM

Cloud Radar (WACR) system, then errors in the quotient $\frac{R^4}{V_w}$ can be reduced to errors in the knowledge

of the antenna beam width¹ and scattering volume range. The beam width can easily be measured to within a tenth of a degree (for MMCR, the antenna beam width is 0.3–0.32 degrees for 6' antennas at most sites and 0.19 degrees for 10' antenna at SGP). Thus, it is estimated that the factor θ_{3dB}^2 is accurate to within 0.3 dB. Assuming that the range accuracy is +/- half a range gate (45 meters), the error in reflectivity due to range errors is less than 0.4 dB at 1 km (0.6 dB at 500 m/0.2 dB at 2 km).

1.2.2 Transmit Power Measurement Error

MMCR transmit power is monitored by the software. If the transmit power is within certain limits (unknown) of the initial transmit power, then the software adjusts the reported dBZ values for changes in transmit power. If the power falls outside this range, then no adjustment is made. Assuming that the software adjusts the power correctly, the estimated error for variation in transmit power is < 0.25 dB.

¹ This assumes that the antenna's two-way pattern is close to Gaussian, which is very likely to be the case, unless the antenna is damaged.

1.2.3 Receiver Gain Fluctuations

Receiver gain fluctuations are not accounted for by the MMCR processing software. A Ka-band noise diode built into MMCR is used to inject a test signal to estimate receiver gain and noise figure. An analysis of receiver gain stability using the MMCR daily calibration data is summarized in Table 1 for periods between maintenance activities. These data show that receiver gain fluctuations can be as large as 1.4 dB, though the standard deviation of the gain error is less than 0.5 dB in all cases.

Table 1. Receiver gain minimum, maximum, and standard deviation for the Boundary-Layer mode for the five MMCR installations.

	SGP	Barrow	Darwin	Manus	Nauru
Min Gain (dB)	52.5	59.3	65.7	69.6	51.5
Max Gain (dB)	53.4	60.5	66.1	69.9	53.2
Deviation from initial calibration (dB)	+0.4/-0.5	+0.3/-0.9	+0.1/-0.3	+0.1/-0.2	+0.3/-1.4
Standard Deviation (dB)	0.19	.21	.06	0.08	.47

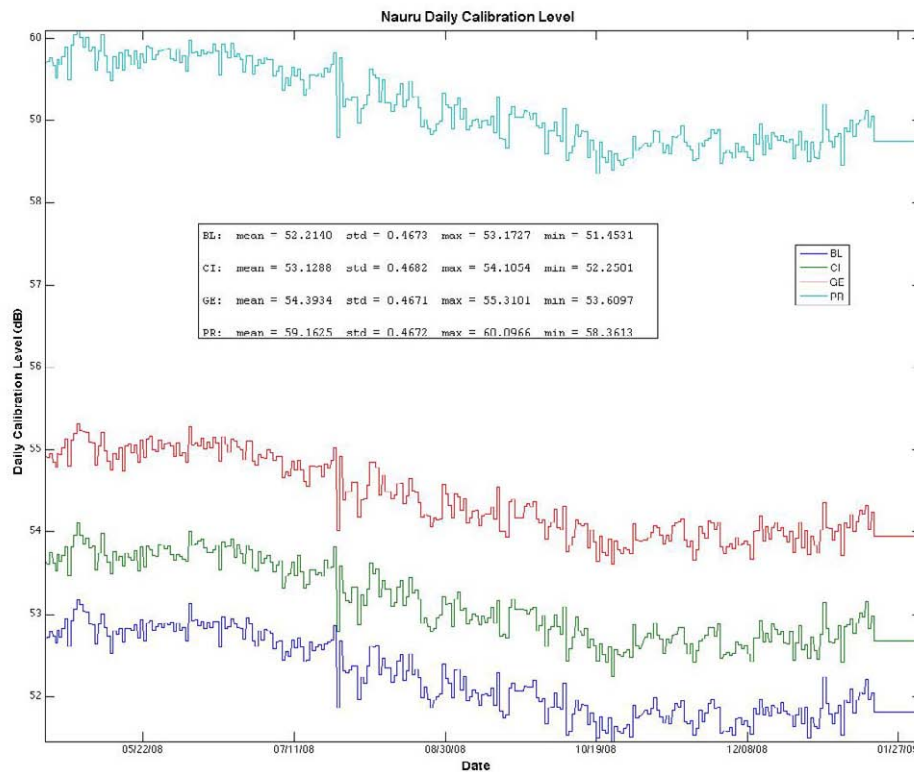


Figure 1. Nauru daily calibration showing drift of +0.3 to -1.4 dB from the initial calibration values.

1.2.4 Received Power Measurement Errors

The following error mechanisms can potentially contribute to power measurement errors:

- Errors in the zeroth moment estimator that extracts signal power from the measured Doppler spectrum
- Errors in the transfer function used to map measured power into calibrated power. This is a problem that has been identified with MMCR.

1.2.4.1 Antenna Gain Measurement Error

The gain of the MMCR antennas was measured initially by the manufacturer and is assumed to have been stable throughout the lifetime of the antenna (approximately 15 years). The initial gain measurement accuracy is thought to be no better than 1.0 dB. The amount of gain variation due to aging of the antenna is unknown.

1.2.4.2 Zeroth Spectral Moment Estimator

Both WACR and MMCR use moment estimators to extract the zeroth, first, and second moments of the Doppler spectrum. At low signal-to-noise ratio the zeroth moment, corresponding to P_r in the range equation, can be biased either upward or downward, depending on the signal's spectral width relative to spectral resolution. Figure 2 plots zeroth-moment bias for the MMCR cirrus mode as a function of the spectral peak signal-to-noise ratio for three cases: 0.2, 0.6, and 2.0 m/s spectral width.

To explain this behavior, consider the following conditions. If the signal spectrum is below the noise, then the moment estimator will overestimate signal power, since it treats noise peaks as signal, even if no signal is present. If the spectrum is broad (relative to the spectral resolution) and slightly above the noise floor, then the moment estimator will underestimate signal power. This is because there is significant power in the signal spectrum that falls below the noise floor and is therefore ignored when computing the zeroth moment.

The standard deviation of the zeroth-moment estimate is plotted as a function of the spectral peak signal-to-noise ratio in Figure 3 for three different spectral widths. As expected, the standard deviation is seen to be large for low signal-to-noise ratios. However, the standard deviation is not strongly dependent on spectral width.

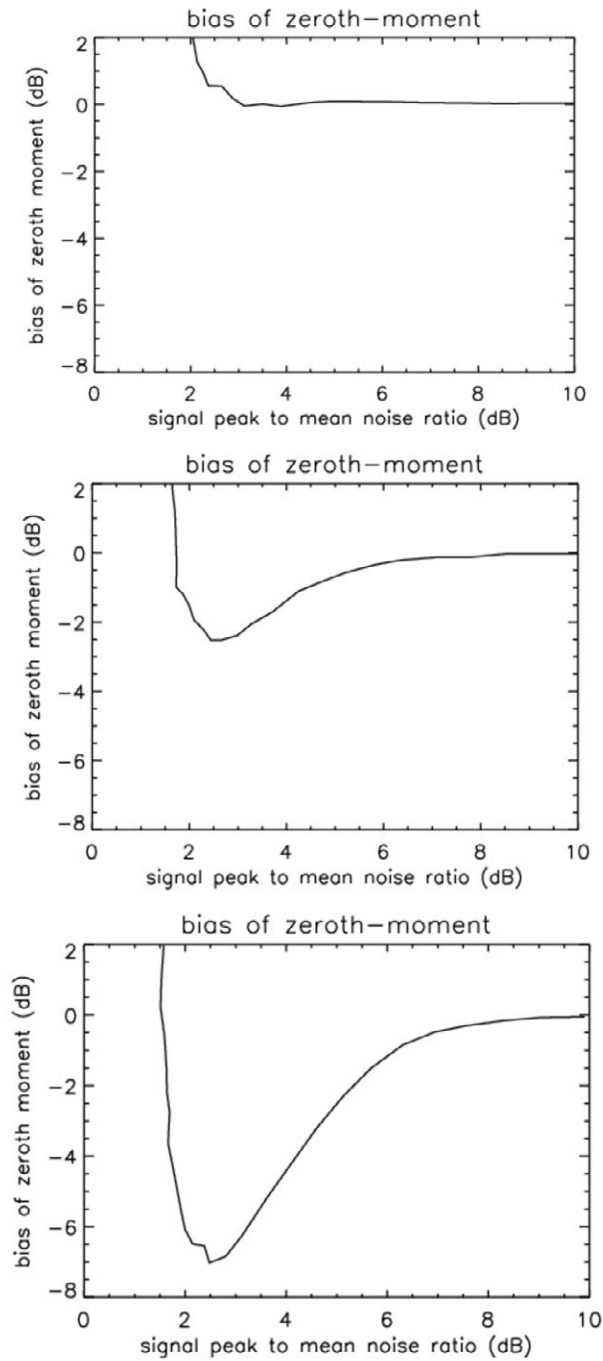


Figure 2. Simulated bias of the zeroth spectral moment (P_r) as a function of the peak signal-to-mean-noise floor level for three spectral widths: 0.2 m/s (top), 0.6 m/s (middle), and 2.0 m/s (bottom); MMCR CI mode (PRF=7936 Hz, 4 coherent averages), spectral resolution=.066 m/s.

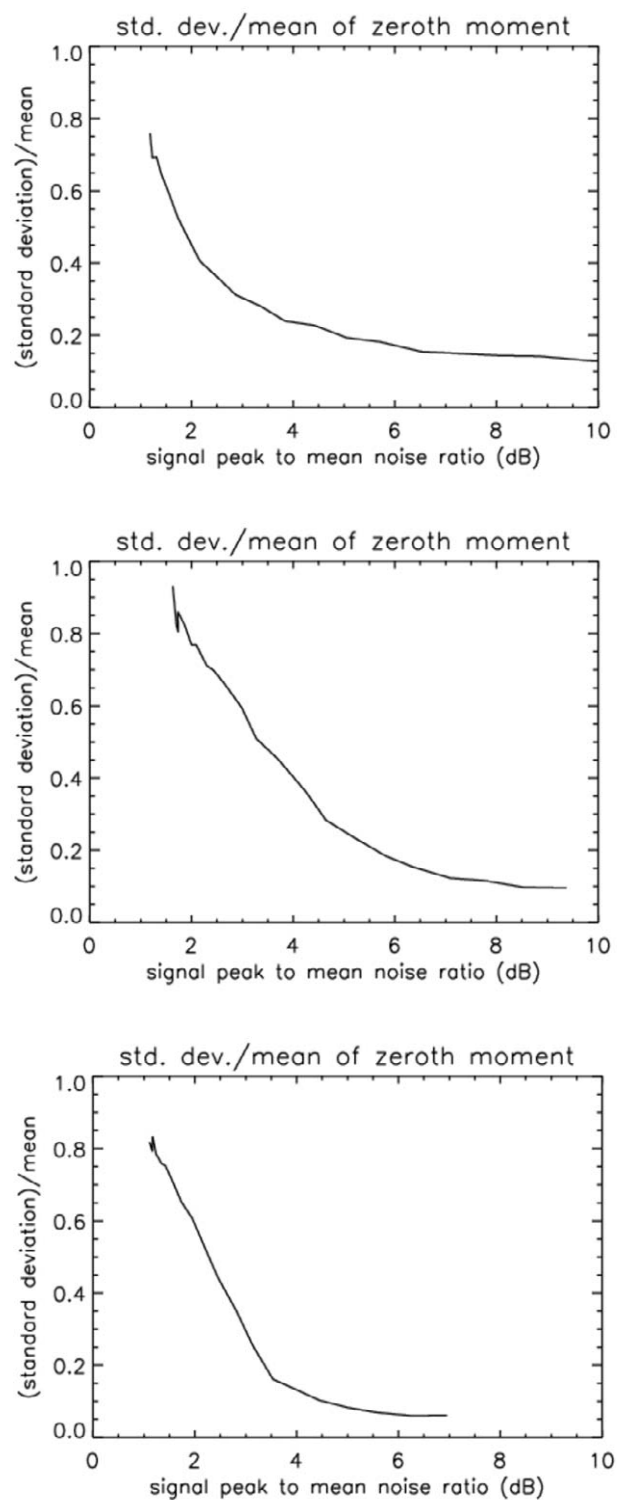


Figure 3. Simulated standard deviation relative to mean of the zeroth spectral moment (P_r) as a function of the peak signal-to-mean-noise floor level for three spectral widths: 0.2 m/s (top), 0.6 m/s (middle), and 2.0 m/s (bottom); MMCR CI mode, spectral resolution=.066 m/s.

1.2.4.3 Bias in the Existing MMCR Receiver Calibration

A typical MMCR receiver transfer function is plotted in Figure 4. The transfer function exhibits significant saturation for input power levels above -70 dBm. At input levels below -120 dBm, the displayed transfer function is modified to account for the presence of receiver noise. However, the true transfer function remains highly linear for input power levels falling below -75 dBm.

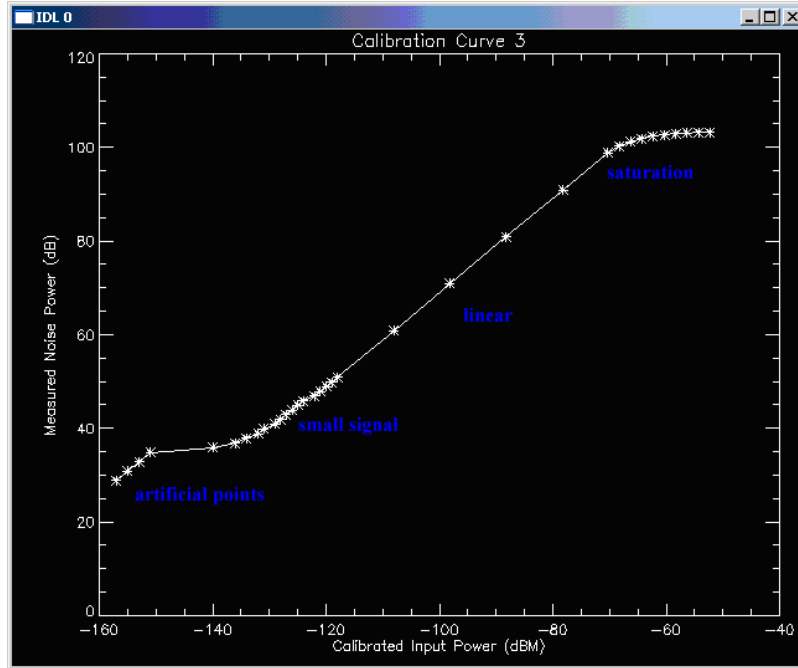


Figure 4. Typical MMCR receiver transfer function.

The transfer function is generated using the following steps (taken from an existing MMCR calibration document):

- The lower left portion contains a series of artificial points that are inserted into the curve to prevent very small (often erroneous) signals from producing errors in the computation of reflectivity². The small signal region is computed from a measurement of both the receiver noise level and the calibration signal of the calibrated signal source (noise diode).
- The saturated region is measured by injecting a high-level signal at 60 MHz into the IF section of the receiver. (The IF section is the first to saturate as it has the most gain.)

According to this same document, the transfer function in Figure 4 is used to convert the total power in the Doppler spectrum (the zeroth moment of the Doppler spectrum) to a calibrated power level in dBm. This procedure is correct if the signal statistics of the calibration signal are identical to those of the cloud signal. However, it will lead to a bias if the statistics are different. This is the case in the saturation region, where a high-level sinusoidal signal was used to calibrate the receiver IF.

² The high positive slope in this region actually enhances the effect of weak signals, as seen in Figure 2.

1.3 Simulated Bias

Simulated output signals from the MMCR receiver were generated using a typical MMCR transfer function from the SGP MMCR³. In the forward direction, the transfer function was modified to be linear in the small signal region, which is true of the actual transfer function. A bivariate Gaussian white noise signal with varying mean power was generated to simulate a cloud signal. An additional noise signal was generated at -137.0 dBm to simulate the receiver noise contribution. The combined signal plus noise was passed through the receiver transfer function, averaged to a mean power, and finally converted back to an estimate of mean input power by applying the inverse of the calibration curve, now including the noise bias factor for small signals.

The error resulting from this process is shown in Figure 5. Note that the calibration curve allowed signals to be extracted from the noise down to a level of approximately -143 dBm (6 dB below the noise). However, for input signals between -65 and -52 dBm, the corrected measured power is biased downward, with as much as 5 dB error. Expressed mathematically, the desired mean value of the calibrated input power, \bar{p}_i , is given by

$$\bar{p}_i = E[T^{-1}(p_m)] \quad (1)$$

where T^{-1} is the inverse of the receiver transfer function (i.e., the calibration curve), p_m is a vector of the measured signal power, and $E[\]$ is the expected value operator. In general, $\bar{p}_i \neq T^{-1}(E[p_m])$, which is how the current calibration process is implemented.

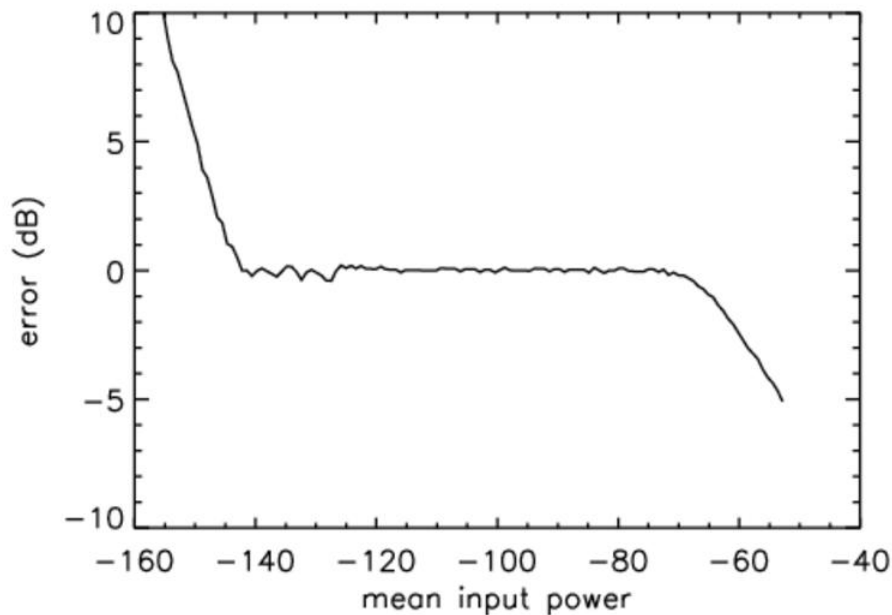


Figure 5. Mean input power estimation error using transfer function applied after computing the mean measured power.

³ sgpmmclogC1.00.20070627.000000.raw.20071780000CalTable.nc

1.3.1 Temperature Dependence on the Index of Refraction of Water

The scattering cross-section of small droplets is dependent on the value K , which is a function of the droplet index of refraction, n [1, eq. 5.73]:

$$K = \frac{n^2 - 1}{n^2 + 2}$$

The index of refraction of water is a function of frequency and temperature [1, Section E-2, pg. 2020]. This formulation was used to compute $|K|$ at 35.0 GHz as a function of temperature (Figure 6), which shows a variation of 0.14 dB at 35.0 GHz. Since reflectivity is dependent on $|K|^2$, uncompensated temperature variations map into a .2 dB reflectivity error at 35.0 GHz. The current software assumes $|K| = .964$.

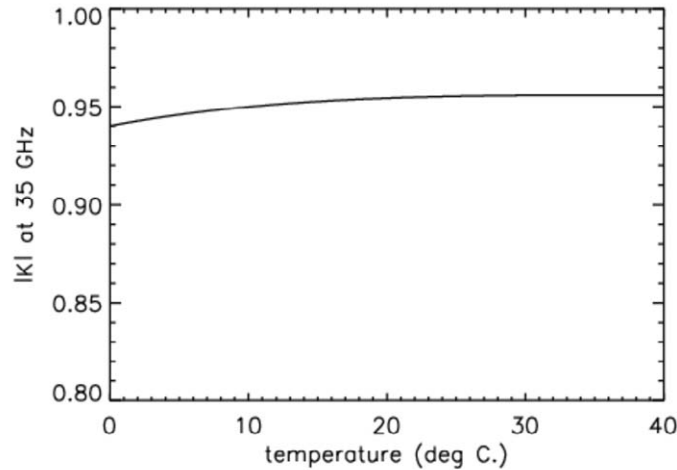


Figure 6. Temperature dependence of $|K|$ at 35 GHz.

1.3.2 Propagation Losses

The current MMCR reflectivity data are not compensated for propagation losses. Propagation losses at Ka-band arise from water vapor absorption and extinction due to hydrometeors.

1.3.2.1 Attenuation due to Atmospheric Water Vapor

The total atmospheric loss factor from the ground through the top of the atmosphere is given by [Waters 1976]:

$$\tau_0(dB) = 0.17 + .013\rho_0(g/m^3) \text{ at 35 GHz.}$$

At 35 GHz, the range of zenith attenuation is from .17 dB to 0.5 dB (low to high humidity). Most of this attenuation will occur in the boundary layer, where water vapor is concentrated. Thus, high clouds could experience as much as 1.0 dB two-way loss at Ka-band.

1.3.2.2 Attenuation Due to Hydrometeors

The extinction coefficient due to small liquid water droplet (Rayleigh approximation) is given by [1, eq. 5.105].

$$\kappa_1 = .434 \frac{6\pi}{\lambda_0} \text{Im}(-K) \text{ dB/km/g/m}^3.$$

For a wet cloud (1 g/m³), κ_1 ranges from 0.45 to 1.1 dB/km at Ka-band (.45 dB at 40C, 1.1 dB at 0C). The two-way loss will be double this amount.

Loss in ice or snow is negligible at Ka-band.

1.3.2.3 Antenna/Radome Losses

Signal loss due to absorption and scattering from sheeting water on a radome can be significant. Lab measurements carried out at ProSensing at W-band showed that a low-to-moderate density of small droplets had minimal effect (less than 0.5 dB). However, when the droplet density becomes large with some regions of sheeting, the one-way loss was found to be 2–3 dB (4–6 dB two-way loss). It is expected that this effect will be reduced considerably at Ka-band.

1.4 Summary of Error Sources

Table 2 summarizes the various calibration error sources considered in this report. This table indicates that total calibration error should be small (< 3 dB) for clouds above 10 dB SNR.

Reflectivity bias at low SNR occurs due to errors in the moment estimator. This error is particularly pronounced when the cloud spectral width is large compared to the Doppler spectral resolution. The errors show up as both a bias and an increase in the standard deviation of the error, with the bias being largest at a ratio of 2.5 dB spectral peak power to mean spectral noise power ratio.

Table 2. Summary of calibration error sources in WACR.

Error Source	Error in reported MMCR reflectivity
Antenna Gain	1.0 dB uncertainty in gain measured by manufacturer; more if antenna becomes damaged
Transmit Power Fluctuations	< 0.25 dB when tracked and accounted for in reported dBZ; can be significantly higher if power drops outside established limits (need to know limit)
Receiver Gain Fluctuations	< 1.5 dB max for all radars; typically less than 0.5 dB (see Table 1); not accounted for in reported dBZ
Scattering volume/range errors	< .3 dB antenna pattern uncertainty < .4 dB at 1-km range gate uncertainty
Receiver power Measurement	Up to 5 dB at extremes of dynamic range due to transfer function errors (Figure 5) Up to 7 dB at low SNR due to errors in moment estimation (Figure 2)
Index of refraction of water	.2 dB over temperature (no error at 40C; 0.2 dB at 0° C)
Propagation effects (2-way)	Water vapor: up to 1.0 dB for high clouds Liquid water: 2.2 dB/km for 1g/m ³ liquid cloud Water on radome: need to estimate or test

1.4.1 References

1. Ulaby, FT, RK Moore, and K Fung. 1986. *Microwave Remote Sensing, Active and Passive, Volume I and II*. Artech House, Norwood, MA.
2. Doviak, RJ and DS Zrnic. 1993. *Doppler Radar and Weather Observations, 2nd Edition*. Academic Press, San Diego, equation 4.15.
3. Probert-Jones, JR. 1962. "The radar equation in meteorology." *Journal of the Royal Meteorological Society* 88: 485-495.
4. Craeye, C, P Sobieski, E Robin, and A Guissard. 1997. "Angular errors in trihedrals used for radar calibrations." *International Journal of Remote Sensing* 18(12): 2683-2689.
5. Robertson, SD. 1947. "Targets for microwave radar navigation." *Bell System Technical Journal* 26: 852-869.
6. WACR SGP Operations Manual, June, 2005, Table 5.
7. Waters, JW. 1976. "Absorption and emission of microwave radiation by atmospheric gases." In *Methods of Experimental Physics*. M.L. Meeks, ed., 12, Part B, Radio Astronomy, Academic Press, Section 2.3.



U.S. DEPARTMENT OF
ENERGY